PHYSICAL REVIEW B **86**, 195304 (2012)

Observation of a highly spin-polarized topological surface state in $GeBi_2Te_4$

K. Okamoto,[1] K. Kuroda,[1] H. Miyahara,[1] K. Miyamoto,[2] T. Okuda,[2] Z. S. Aliev,[3] M. B. Babanly,[3] I. R. Amiraslanov,[4] K. Shimada,[2] H. Namatame,[2] M. Taniguchi,[1,2] D. A. Samorokov,[5] T. V. Menshchikova,[5] E. V. Chulkov,[6,7] and A. Kimura[1,*]

[1]*Graduate School of Science, Hiroshima University, 1-3-1 Kagamiyama, Higashi-Hiroshima 739-8526, Japan*

[2]*Hiroshima Synchrotron Radiation Center, Hiroshima University, 2-313 Kagamiyama, Higashi-Hiroshima 739-0046, Japan*

[3]*General and Inorganic Chemistry Department, Baku State University, AZ1148 Baku, Azerbaijan*

[4]*Institute of Physics, Azerbaijan National Academy of Science, AZ1143 Baku, Azerbaijan*

[5]*Laboratory of Nanostructured Surfaces and Covers, Tomsk State University, 634050 Tomsk, Russia*

[6]*Departamento de Física de Materiales UPV/EHU, Centro de Física de Materiales CFM, and Centro Mixto CSIC-UPV/EHU, 20080 San Sebastián/Donostia, Basque Country, Spain*

[7]*Donostia International Physics Center, 20018 San Sebastián/Donostia, Basque Country, Spain*

(Received 9 July 2012; revised manuscript received 15 October 2012; published 6 November 2012)

Spin polarization of a topological surface state for $GeBi_2Te_4$, the newly discovered three-dimensional topological insulator, has been studied by means of state-of-the-art spin- and angle-resolved photoemission spectroscopy. It has been revealed that the disorder in the crystal has a minor effect on the surface-state spin polarization, which is 70% near the Dirac point in the bulk energy gap region (~180 meV). This finding promises not only to realize a highly spin-polarized surface-isolated transport but also to add functionality to its thermoelectric and thermomagnetic properties.

DOI: 10.1103/PhysRevB.86.195304 PACS number(s): 73.20.−r, 79.60.−i

I. INTRODUCTION

Topological insulators (TIs) have recently emerged as a new state of quantum matter and are distinguished from conventional insulators by a massless Dirac cone surface state in the bulk energy gap, the so-called topological surface state (TSS). The spin orientation of the TSS is locked with respect to crystal surface momentum, resulting in a helical spin texture.[1,2] The unique properties of topological surface electrons provide fertile ground to realize new electronic phenomena, such as a magnetic monopole arising from the topological magnetoelectric effect and Majorana fermions at the interface with a superconductor.[3,4] Due to time-reversal symmetry, a TSS is protected from backscattering in the presence of a weak perturbation, a feature which is required for the realization of dissipationless spin transport in the absence of external magnetic fields in novel quantum devices.[5,6]

A number of materials that hold spin-polarized TSSs have been intensively studied, such as $Bi_{1-x}Sb_x$,[7,8] Bi_2Se_3,[9–12] Bi_2Te_3,[13,14] and thallium- and lead-based ternary compounds.[15–23] Among these materials, Bi_2Se_3 has been regarded as the most promising three-dimensional (3D) TI because it possesses a single TSS in a rather wide bulk energy gap.[9,10] However, no surface-isolated conduction has been observed for this binary compound even with the low carrier density realized by the hole doping.[24–26] One of the reasons for the dominant bulk conductance might be ascribed to its band structure, where the Dirac point of the topological surface state is located at or below the bulk valence-band maximum. Actually, the surface-to-bulk scattering has been directly observed by scanning tunneling microscopy.[12]

A homologous series of pseudobinary compounds, nGeTe-$m$$Bi_2Te_3$, was intensively studied in terms of its thermoelectric, galvanomagnetic, and thermomagnetic properties.[27–30] Among them, $GeBi_2Te_4$ was theoretically proposed as a member of the 3D TIs.[31–33] It was experimentally verified to be a 3D TI possessing a single TSS by an angle-resolved photoemission spectroscopy (ARPES) experiment.[34] The crystal structure of $GeBi_2Te_4$ assumed in the calculation was composed of seven-layer (7L) blocks formed by the atomic layer sequence Te-Bi-Te-Ge-Te-Bi-Te, as shown in Fig. 1(a). However, the structure in the *real* material was found to deviate from the ideal one. It was revealed by an x-ray diffraction study that the central cation layer of the 7L block is not pure Ge but contains equal amounts of randomly distributed Ge and Bi atoms, and the other two cation layers result also in a substantial intermixing[35] [Fig. 1(b)]. This observation prompts the important question of how the spin polarization of the TSS would be affected by the intermixing in the $GeBi_2Te_4$ crystal.

Revealing the size of the bulk energy gap and the **k**-space location of the TSS, especially with respect to the bulk band gap, is crucial for realizing topological transport with a sufficiently isolated surface conduction. Also, the surface spin polarization needs to be as high as possible even though its magnitude is predicted to be reduced to 50%–60% for Bi_2Se_3 and Bi_2Te_3 due to inevitable spin and orbital entanglement.[36] Although the topological surface state was experimentally identified,[34] such important information on these aspects in the presence of mixed interlayers is so far missing for $GeBi_2Te_4$. Here, we report that the Dirac point of the TSS is located within the bulk band gap of ~180 meV and that the TSS has a substantial spin polarization of ~70%, which is revealed by means of spin-resolved/integrated ARPES. This finding promises to realize a surface-isolated, highly spin-polarized transport and add functionality to its thermoelectric and thermomagnetic properties.

II. EXPERIMENT

A single crystalline ingot of $GeBi_2Te_4$ was grown by the vertical Bridgman-Stockbarger method. The grown crystal was characterized by x-ray diffraction using a Bruker D8 ADVANCE diffractometer with Cu K_α radiation. Spin-integrated ARPES measurement was carried out with synchrotron radiation at the linear undulator beam line (BL-1) of

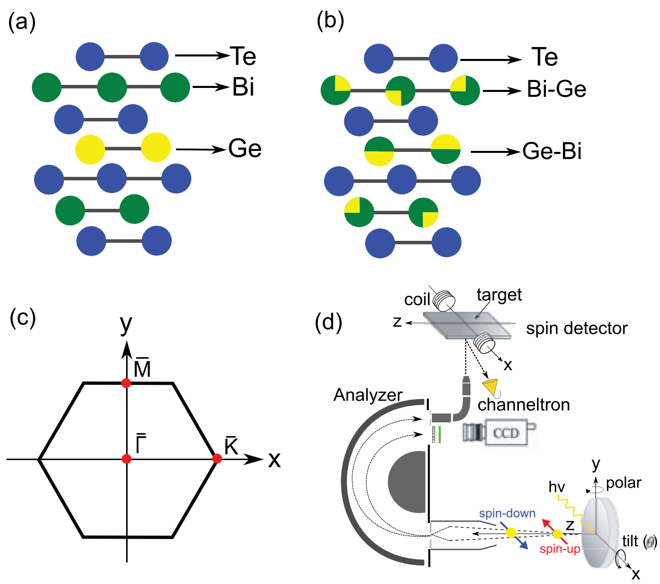

FIG. 1. (Color online) (a) Ideal and (b) experimentally determined seven-layer blocks of $GeBi_2Te_4$ crystal (see text). (c) Surface Brillouin zone. (d) Experimental geometry for spin-ARPES measurement.

the Hiroshima Synchrotron Radiation Center (HiSOR). The spin-resolved ARPES (SARPES) experiment was performed with a He discharge lamp ($h\nu = 21.22$ eV) at the Efficient SPin REsolved SpectroScOpy (ESPRESSO) end station with the very-low-energy-electron-diffraction (VLEED)-type spin polarimeter.[37] The spin polarimeter utilizes [Fig. 1(d)] a magnetic target of a Fe(001)-$p(1\times1)$-O film grown on a MgO(001) substrate, which achieves a 100 times higher efficiency compared to those of conventional Mott-type spin detectors.[37] Photoelectron spin polarizations were measured by switching the direction of in-plane target magnetizations. This simultaneously eliminated any instrumental asymmetry, which is a great advantage for the quantitative spin analysis of nonmagnetic systems, as in the present case. The angle of light incidence was 50° relative to the lens axis of the electron analyzer. The sign of the polar (tilt) angle is defined as positive in the case of a clockwise (anticlockwise) rotation about y axis (x axis), as shown in Fig. 1(d). The energy and wave-number resolutions for the synchrotron radiation ARPES (BL-1) were set to better than 48 meV and 0.05 Å^{-1}, respectively, while those for the ARPES (SARPES) with a He discharge lamp were set to 19 meV and <0.036 Å^{-1} (27 meV and <0.06 Å^{-1}). The measurement temperatures at BL-1 and at the ESPRESSO end station were 10 and 50 K, respectively. The samples were cleaved *in situ* under an ultrahigh vacuum below 1×10^{-8} Pa.

III. RESULTS AND DISCUSSION

Figures 2(a) and 2(b) show the ARPES energy dispersion curves along the $\bar{\Gamma}\bar{M}$ and $\bar{\Gamma}\bar{K}$ lines of the surface Brillouin zone (SBZ) [Fig. 1(c)], respectively. Two surface energy bands, i.e., a TSS with a crossing point at a binding energy E_B of 260 meV (Dirac point), are clearly seen along these lines. The bulk conduction band (BCB) is enclosed by the TSS and crosses the Fermi energy E_F with a substantial photoemission intensity. This feature is a little different from what is observed in the former ARPES study on the same material,[34] which might be due to a slight difference in the degree of intermixing effect. The reasons for the n-type conductivity of this compound are discussed and ascribed to the predominance of the substitutional Bi_{Ge} defects, favored by the existence of mixed cation layers in their structures, or to V_{Te} anion vacancies.[29] Constant energy contours in the $\mathbf{k}_\parallel$ range -0.25 Å$^{-1} \leqslant k_x, k_y \leqslant +0.25$ Å^{-1} from -200 to $+250$ meV with respect to the Dirac point ($E_B = 260$ meV) are shown in Fig. 2(c). A hexagonally shaped constant energy contour is observed at E_F, whose shape is preserved even at $E_B = 150$ meV. The hexagon of the TSS evolves into the pointlike feature at the Dirac point and is again strongly deformed into a snowflake below the Dirac point. Another triangular feature is enclosed within the TSS at E_F, which comes from the bulk conduction band. These features are consistent with the previous ARPES experiment.[34] Here it has to be mentioned that the size of the constant energy contour of $GeBi_2Te_4$ ($|k_x| \sim 0.1$ Å^{-1} at 150 meV above the Dirac point) is almost twice that of the *ordered* Bi_2Se_3 ($\sim$0.05 Å^{-1} at the same energy).[10] This result implies that the intermixing of the $GeBi_2Te_4$ crystal would broaden the momentum width of the TSS.

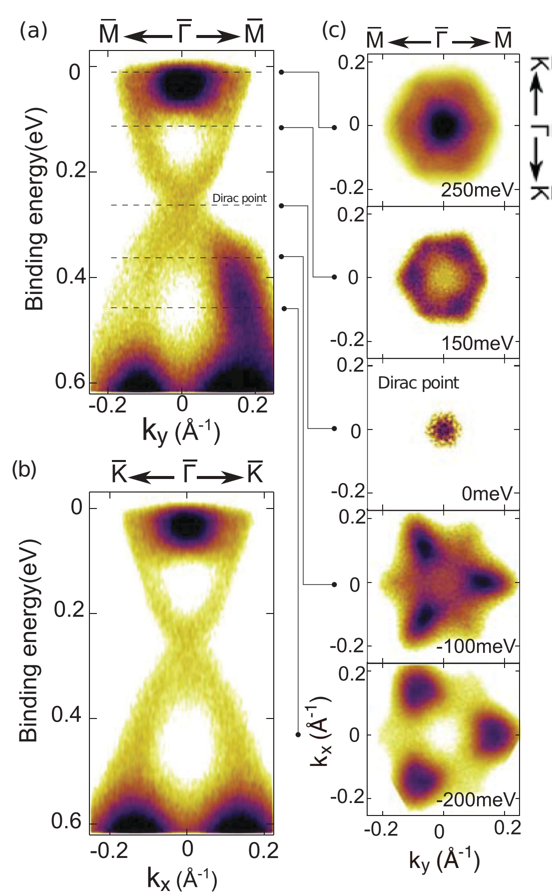

FIG. 2. (Color online) (a) Experimental ARPES results for $GeBi_2Te_4$. Energy dispersion curve along the (a) $\bar{\Gamma}\bar{M}$ and (b) $\bar{\Gamma}\bar{K}$ lines. (c) Constant energy surfaces at 250, 150, 0, -100, and -200 meV with respect to the Dirac point ($E_B = 260$ meV).

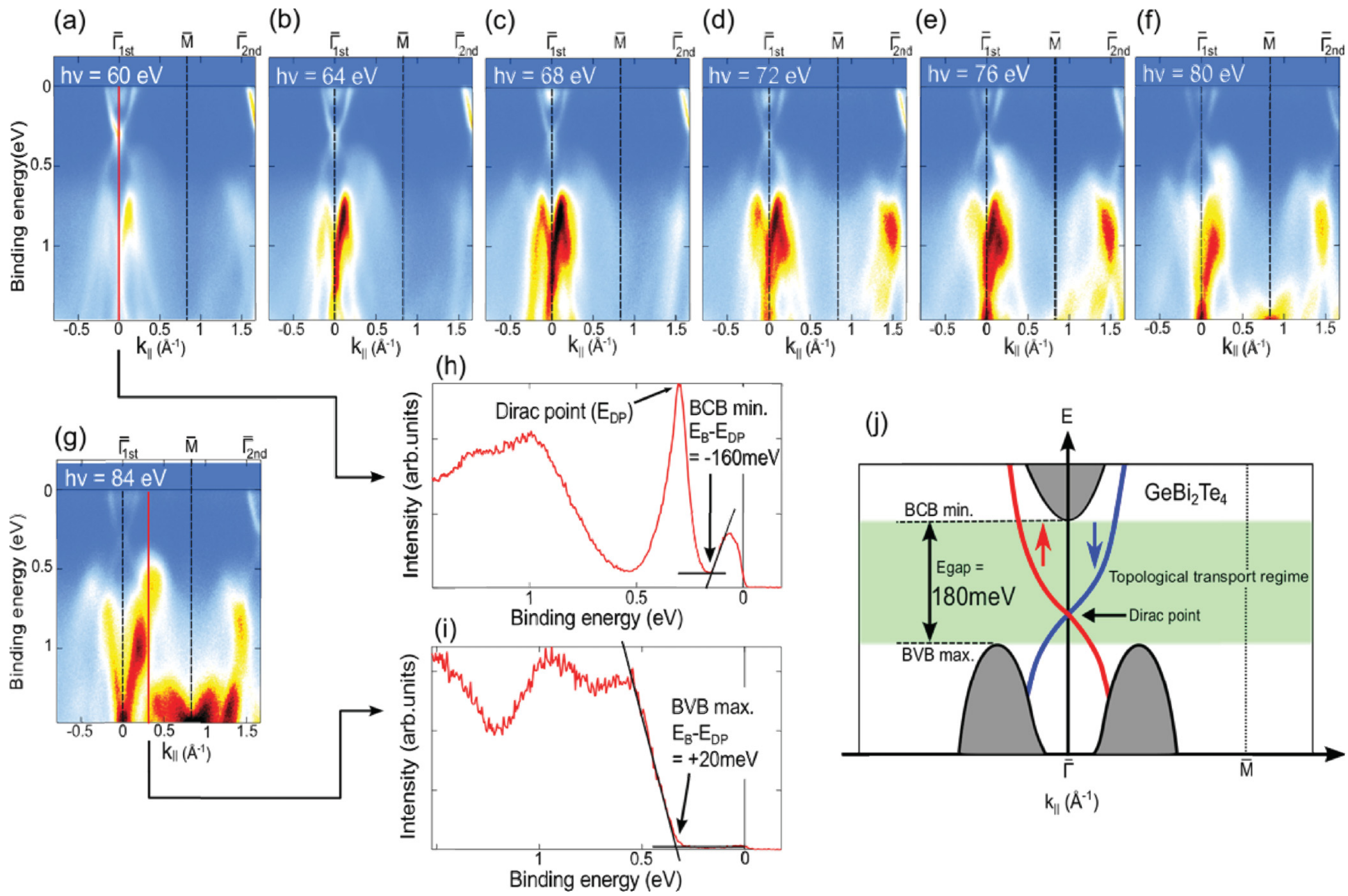

FIG. 3. (Color online) ARPES E-$k_{\parallel}$ map over a wide $k_{\parallel}$ range along the $\bar{M}\bar{\Gamma}\bar{M}$ line acquired at $h\nu =$ (a) 60, (b) 64, (c) 68, (d) 72, (e) 76, (f) 80, and (g) 84 eV. Energy distribution curves in the E_B range of 0–1.4 eV sliced along the constant $k_{\parallel}$ lines at (h) 0 Å^{-1} for $h\nu = 60$ eV and (i) 0.3 Å^{-1} for $h\nu = 84$ eV. (j) Schematics of surface (blue and red lines) and bulk band structures (gray shaded area) of $GeBi_2Te_4$ figured out from the present experimental results.

To determine the **k**-space location of the bulk states with respect to the TSS, we have performed a detailed photon energy dependence study over a wide $k_{\parallel}$ range. The ARPES measurements were performed with several incident photon energies $h\nu$ from 60 to 84 eV to cover the whole Brillouin zone along the k_z direction. Figures 3(a)–3(g) show the E-$k_{\parallel}$ map over a wide $k_{\parallel}$ range along the $\bar{M}\bar{\Gamma}\bar{M}$ line acquired at $h\nu = 60$–84 eV. The surface states at the $\bar{\Gamma}$ points in the first ($\bar{\Gamma}_{1st}$) and second ($\bar{\Gamma}_{2nd}$) SBZs are found to be identical, which signifies a single TSS in this compound. The Dirac point energy does not change with $h\nu$ except for a time-dependent energy shift, as will be discussed later, while the bulk states do, which again confirms their respective two- and three-dimensional natures. At $h\nu = 60$ eV, the BCB enclosed by the TSS is clearly identified. In going to higher $h\nu$ it gradually shifts towards E_F and almost vanishes finally at $h\nu = 84$ eV. The bulk valence band (BVB), on the other hand, gradually grows up and shifts to lower E_B with increasing $h\nu$, achieving its maximum (minimum in E_B) at $h\nu = 84$ eV.

Figures 3(h) and 3(i) show the energy distribution curves (EDCs) in the E_B range of 0–1.4 eV sliced along the constant $k_{\parallel}$ lines at 0 Å^{-1} for $h\nu = 60$ eV and 0.3 Å^{-1} for $h\nu = 84$ eV. In Fig. 3(h), a sharp peak is observed at the Dirac point energy ($E_B = 300$ meV), and the BCB exhibits a Fermi energy cutoff accompanying a higher E_B tail. The slightly higher Dirac point energy than that observed for Fig. 2 (different set of measurements) might be due to the slightly different sample stoichiometry. Here, the BCB minimum is found at $E_B = 140$ meV (160 meV above the Dirac point) by extrapolating the higher-energy tail to "zero" intensity with a linear function. To determine the BVB maximum, another EDC is given in Fig. 3(i) and shows a monotonic decrease in intensity with decreasing E_B. By applying a similar fitting procedure to that used for the BCB, the BVB maximum energy is estimated to be $E_B = 340$ meV. Since, as is commonly observed for Bi_2Se_3,[38] the 20 meV time-dependent energy shift to higher E_B occurs at the same time as that of the TSS, one may assume that the BVB maximum is located at 20 meV below the Dirac point. Thus these results lead to the conclusion that the total energy gap between the BVB maximum and BCB minimum is 180 meV in $GeBi_2Te_4$. An important finding is that the Dirac point of TSS is located inside this indirect bulk energy gap (20 meV above the BVB maximum and 160 meV below the BCB minimum), as schematically shown in Fig. 3(j).

To unveil the spin characteristics of the TSS, the SARPES experiment was carried out. Two spin-integrated energy dispersion curves measured with a He discharge lamp ($h\nu = 21.22$ eV) near the $\bar{\Gamma}$ point in the first and the second SBZs

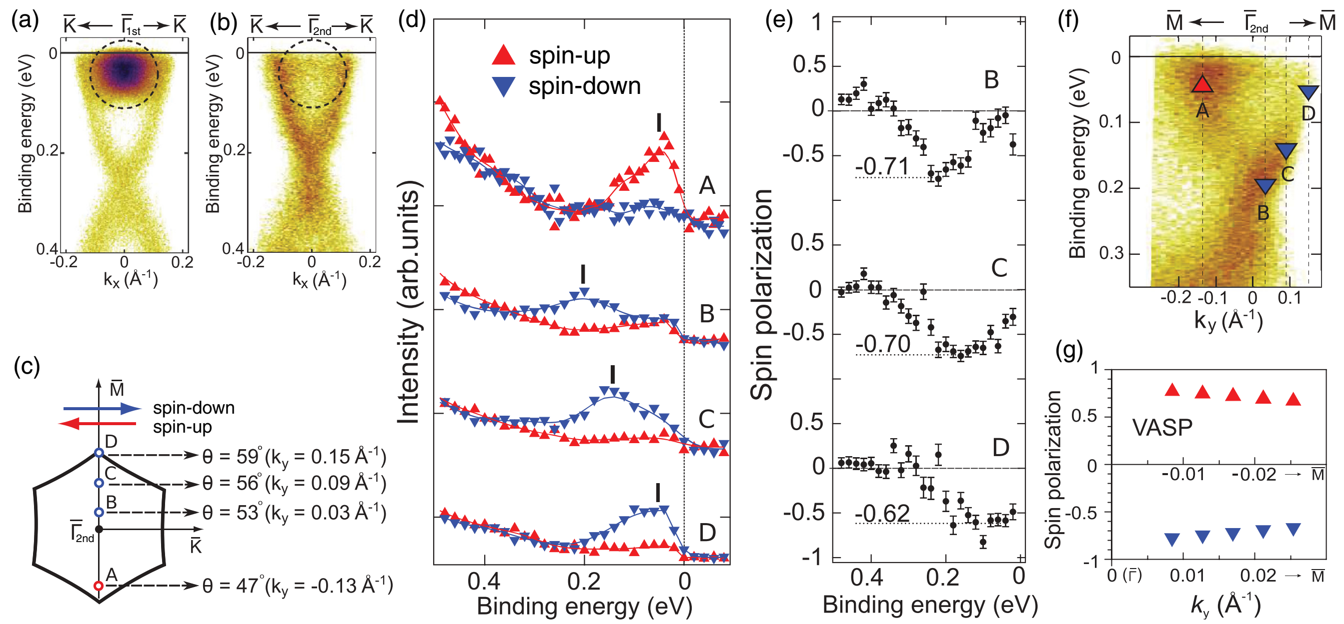

FIG. 4. (Color online) Spin-integrated energy dispersion curves acquired with a He discharge lamp ($h\nu = 21.22$ eV) along $\bar{K}\bar{\Gamma}\bar{K}$ in the (a) first SBZ and (b) second SBZ. Note here that bulk conduction band intensity is suppressed compared with that in the first SBZ, as highlighted by dashed circles. (c) Schematic of constant energy contour at $E_B = 50$ meV is shown with a black solid line and $k_\parallel$ points (A–D) for spin-resolved measurements are denoted with blue and red circles. Measured spin-polarization directions are also shown with arrows. (d) Spin-resolved energy distribution curves of $GeBi_2Te_4$ for emission angles θ of 47° (A), 53° (B), 56° (C), and 59° (D) and (e) corresponding spin polarizations. (f) ARPES results along $\bar{M}\bar{\Gamma}\bar{M}$ in the second SBZ. The contour plot has superimposed triangles pointing up and down, indicating the spin character of the corresponding spectral features, as derived from spin-resolved spectra in (d). (g) Theoretical spin-polarization values as a function of wave number obtained from the VASP first-principles calculation for *ordered* $GeBi_2Te_4$.

are compared in Figs. 4(a) and 4(b). In Fig. 4(a), a significant overlap of the bulk conduction band intensity is recognized at the first SBZ, while the bulk-derived spectral intensity is well suppressed at the second SBZ, as can also be seen in Fig. 4(b). It is apparent that it would be better to choose the second SBZ with larger emission angles for a quantitative spin analysis since the overlap of the TSS with the BCB can be avoided. Figure 4(d) shows the spin-resolved EDCs of $GeBi_2Te_4$ at emission angles of 47°, 53°, 56°, and 59°, where the respective $k_\parallel$ values are −0.13, 0.03, 0.09, and 0.15 Å^{-1} with respect to the $\bar{\Gamma}_{2nd}$ point ($k_\parallel = 1.66$ Å^{-1}), as denoted by A–D in Fig. 4(c). The measured spin polarizations are in plane and orthogonal to $\mathbf{k}_\parallel$, as expected for the helical spin texture of topological surface states [Fig. 4(c)]. Here, the spin-up and spin-down spectra are plotted with triangles pointing up and down, respectively. At $\theta = 59°$ (D), the spin-down intensity is predominant and crosses E_F, while the spin-up intensity is quite small and featureless. On the other hand, at $\theta = 47°$ (A), which corresponds to another TSS branch, the spin-up intensity dominates, with a quite small spin-down intensity near E_F. The observed antisymmetric spin polarization at the two surface-state branches is indeed a manifestation of a 3D TI. The spin-down peak moves to higher E_B with decreasing θ, which parallels the TSS dispersion in the bulk energy gap region [Fig. 4(f)]. The spin polarizations at 59° (D) is about 60% near E_F, and it is enhanced closer to the Dirac point and reaches 70% below 56° (C and B) as shown in Fig. 4(e). Previous experimental works deduced the surface-state spin polarizations of the other 3D TIs only outside the bulk energy gap with rather larger electron momenta. This might be due to insufficient instrumental angular resolutions, and a direct comparison with the present result involving the value in the vicinity of the Dirac point might be difficult. Nevertheless, the observed spin polarization of the TSS for disordered $GeBi_2Te_4$ is very comparable to that calculated for the *ordered* $GeBi_2Te_4$. Figure 4(g) shows theoretical spin polarization for *ordered* $GeBi_2Te_4$ obtained from the VASP[39–42] first-principles calculation. Here, a theoretical spin expectation value as a function of wave number k_y gradually decreases when moving closer to the bottom of the conduction band (∼67%), and it takes the maximum value of ∼77% in the vicinity of the $\bar{\Gamma}$ point. The obtained consistency between theory and experiment indicates that the intermixing of the crystal has only a weak effect on the spin polarization of the TSS.

IV. CONCLUSION

In conclusion, the size of the bulk energy gap for $GeBi_2Te_4$ is determined to be ∼180 meV, and topological surface state below and above the Dirac point are found to be isolated from the bulk band. Importantly, it is revealed that the disorder in the $GeBi_2Te_4$ crystal has a minor effect on the magnitude of the surface-state spin polarization, which shows 70% in the bulk energy gap region. This finding promises to add functionality to the already known interesting thermoelectric and thermomagnetic properties of $GeBi_2Te_4$.

ACKNOWLEDGMENTS

We thank J. Jiang, H. Hayashi, Y. Nagata, and T. Horike for their technical support in the ARPES measurement at BL-1 of the Hiroshima Synchrotron Radiation Center (HiSOR). This work was financially supported by Grant-in-Aid for Scientific Research Kiban A (Grant No. 23244066) and Kiban B (Grant No. 23340105) of the Japan Society for the Promotion of Science (JSPS). The ARPES measurements were performed with the approval of the Proposal Assessing Committee of HSRC (Proposal No. 12-A-24). We also acknowledge partial support from the Basque Country government, Departamento de Educación, Universidades e Investigación (Grant No. IT-366-07), and the Spanish Ministerio de Ciencia e Inovación (Grant No. FIS2010-19609-C02-00).

*akiok@hiroshima-u.ac.jp

[1] L. Fu, C. L. Kane, and E. J. Mele, Phys. Rev. Lett. **98**, 106803 (2007).
[2] L. Fu and C. L. Kane, Phys. Rev. B **76**, 045302 (2007).
[3] M. Z. Hasan and C. L. Kane, Rev. Mod. Phys. **82**, 3045 (2010).
[4] X. L. Qi and S. C. Zhang, Rev. Mod. Phys. **83**, 1057 (2011).
[5] Q. K. Xue, Nat. Nanotechnol. **6**, 197 (2011).
[6] F. Xiu, L. He, Y. Wang, L. Cheng, L. T. Chang, M. Lang, G. Huang, X. Kou, Y. Zhou, X. Jiang, Z. Chen, J. Zou, A. Shailos, and K. L. Wang, Nat. Nanotechnol. **6**, 216 (2011).
[7] D. Hsieh, Y. Xia, L. Wray, D. Qian, A. Pal, J. H. Dil, J. Osterwalder, F. Meier, G. Bihlmayer, C. L. Kane, Y. S. Hor, R. J. Cava, and M. Z. Hasan, Science **323**, 919 (2008).
[8] A. Nishide, A. A. Taskin, Y. Takeichi, T. Okuda, A. Kakizaki, T. Hirahara, K. Nakatsuji, F. Komori, Y. Ando, and I. Matsuda, Phys. Rev. B **81**, 041309 (2010).
[9] Y. Xia, D. Qian, D. Hsieh, L. Wray, A. Pal, H. Lin, A. Bansil, D. Grauer, Y. S. Hor, R. J. Cava, and M. Z. Hasan, Nat. Phys. **5**, 398 (2009).
[10] K. Kuroda, M. Arita, K. Miyamoto, M. Ye, J. Jiang, A. Kimura, E. E. Krasovskii, E. V. Chulkov, H. Iwasawa, T. Okuda, K. Shimada, Y. Ueda, H. Namatame, and M. Taniguchi, Phys. Rev. Lett. **105**, 076802 (2010).
[11] R. C. Hatch, M. Bianchi, D. Guan, S. Bao, J. Mi, B. B. Iversen, L. Nilsson, L. Hornekær, and P. Hofmann, Phys. Rev. B **83**, 241303(R) (2011).
[12] S. Kim, M. Ye, K. Kuroda, Y. Yamada, E. E. Krasovskii, E. V. Chulkov, K. Miyamoto, M. Nakatake, T. Okuda, Y. Ueda, K. Shimada, H. Namatame, M. Taniguchi, and A. Kimura, Phys. Rev. Lett. **107**, 056803 (2011).
[13] Y. L. Chen, J. G. Analytis, J.-H. Chu, Z. K. Liu, S.-K. Mo, X. L. Qi, H. J. Zhang, D. H. Lu, X. Dai, Z. Fang, S. C. Zhang, I. R. Fisher, Z. Hussain, and Z.-X. Shen, Science **325**, 178 (2009).
[14] D. Hsieh, Y. Xia, D. Qian, L. Wray, F. Meier, J. H. Dil, J. Osterwalder, L. Patthey, A. V. Fedorov, H. Lin, A. Bansil, D. Grauer, Y. S. Hor, R. J. Cava, and M. Z. Hasan, Phys. Rev. Lett. **103**, 146401 (2009).
[15] S. V. Eremeev, Yu. M. Koroteev, and E. V. Chulkov, Pis'ma Zh. Eksp. Teor. Fiz. **91**, 664 (2010) [JETP Lett. **91**, 594 (2010)].
[16] S. V. Eremeev, G. Bihlmayer, M. Vergniory, Y. M. Koroteev, T. V. Menshikova, J. Henk, A. Ernst, and E. V. Chulkov, Phys. Rev. B **83**, 205129 (2011).
[17] K. Kuroda, M. Ye, A. Kimura, S. V. Eremeev, E. E. Krasovskii, E. V. Chulkov, Y. Ueda, K. Miyamoto, T. Okuda, K. Shimada, H. Namatame, and M. Taniguchi, Phys. Rev. Lett. **105**, 146801 (2010).
[18] B. Yan, C. X. Liu, H. J. Zhang, C. Y. Yam, X. L. Q. T. Frauenheim, and S. C. Zhang, Europhys. Lett. **90**, 37002 (2010).
[19] H. Lin, R. S. Markiewicz, L. A. Wray, L. Fu, M. Z. Hasan, and A. Bansil, Phys. Rev. Lett. **105**, 036404 (2010).
[20] T. Sato, K. Segawa, H. Guo, K. Sugawara, S. Souma, T. Takahashi, and Y. Ando, Phys. Rev. Lett. **105**, 136802 (2010).
[21] Y. L. Chen, Z. K. Liu, J. G. Analytis, J. H. Chu, H. J. Zhang, B. H. Yan, S. K. Mo, R. G. Moore, D. H. Lu, I. R. Fisher, S. C. Zhang, Z. Hussain, and Z. X. Shen, Phys. Rev. Lett. **105**, 266401 (2010).
[22] K. Kuroda, H. Miyahara, M. Ye, S. V. Eremeev, Yu. M. Koroteev, E. E. Krasovskii, E. V. Chulkov, S. Hiramoto, C. Moriyoshi, Y. Kuroiwa, K. Miyamoto, T. Okuda, M. Arita, K. Shimada, H. Namatame, M. Taniguchi, Y. Ueda, and A. Kimura, Phys. Rev. Lett. **108**, 206803 (2012).
[23] S. Souma, K. Eto, M. Nomura, K. Nakayama, T. Sato, T. Takahashi, K. Segawa, and Y. Ando, Phys. Rev. Lett. **108**, 116801 (2012).
[24] J. G. Analytis, J. H. Chu, Y. Chen, F. Corredor, R. D. McDonald, Z. X. Shen, and I. R. Fisher, Phys. Rev. B **81**, 205407 (2010).
[25] K. Eto, Z. Ren, A. A. Taskin, K. Segawa, and Y. Ando, Phys. Rev. B **81**, 195309 (2010).
[26] N. P. Butch, K. Kirshenbaum, P. Syers, A. B. Sushkov, G. S. Jenkins, H. D. Drew, and J. Paglione, Phys. Rev. B **81**, 241301(R) (2010).
[27] L. E. Shelimova, O. G. Karpinskii, V. S. Zemskov, and P. P. Konstantinov, Inorg. Mater. **36**, 235 (2000).
[28] L. E. Shelimova, O. G. Karpinskii, V. I. Kosyakov, V. A. Shestakov, V. S. Zemskov, and F. A. Kuznetsov, J. Struct. Chem. **41**, 81 (2000).
[29] L. E. Shelimova, P. P. Konstantinov, O. G. Karpinskii, E. S. Avilov, M. A. Kretova, and V. S. Zemskov, J. Alloys Compd. **329**, 50 (2001).
[30] T. Matsunaga, R. Kojima, N. Yamada, T. Fujita, K. Kifune, Y. Kubota, and M. Takata, Acta Crystallogr. Sect. B **66**, 407 (2010).
[31] T. V. Menshchikova, S. V. Eremeev, Yu. M. Koroteev, V. M. Kuznetsov, and E. V. Chulkov, Pis'ma Zh. Eksp. Teor. Fiz. **93**, 18 (2011) [JETP Lett. **93**, 15 (2011)].
[32] S. V. Eremeev *et al.*, Nat. Commun. **3**, 635 (2012).
[33] K. Yang, W. Setyawan, S. Wang, M. B. Nardelli, and S. Curtarolo, Nat. Mater. **11**, 614 (2012).
[34] M. Neupane, S. Y. Xu, L. A. Wray, A. Petersen, R. Shankar, N. Alidoust, C. Liu, A. Fedorov, H. Ji, J. M. Allred, Y. S. Hor, T. R. Chang, H. T. Jeng, H. Lin, A. Bansil, R. J. Cava, and M. Z. Hasan, Phys. Rev. B **85**, 235406 (2012).
[35] O. G. Karpinsky, L. E. Shelimova, M. A. Kretova, and J. P. Fleurial, J. Alloys Compd. **265**, 170 (1998).
[36] O. V. Yazyev, J. E. Moore, and S. G. Louie, Phys. Rev. Lett. **105**, 266806 (2010).
[37] T. Okuda, K. Miyamoto, H. Miyahara, K. Kuroda, A. Kimura, H. Namatame, and M. Taniguchi, Rev. Sci. Instrum. **82**, 103302 (2011).
[38] P. D. C. King *et al.*, Phys. Rev. Lett. **107**, 096802 (2011).
[39] G. Kresse and J. Hafner, Phys. Rev. B **48**, 13115 (1993).
[40] G. Kresse and J. Furthmüller, Comput. Mater. Sci. **6**, 15 (1996).
[41] P. E. Blöchl, Phys. Rev. B **50**, 17953 (1994).
[42] G. Kresse and D. Joubert, Phys. Rev. B **59**, 1758 (1999).